BULLETIN OF THE POLISH ACADEMY OF SCIENCES
TECHNICAL SCIENCES
Vol. 53, No. 3, 2005

Use of body surface potential maps for model-based assessment of local pathological changes in the heart

M. TYŠLER[1]*, M. TURZOVÁ[1], M. TIŇOVÁ[1], J. ŠVEHLÍKOVÁ[1], E. HEBLÁKOVÁ[1], V. SZATHMÁRY[2], and S. FILIPOVÁ[3]

[1]Institute of Measurement Science, Slovak Academy of Sciences, Dúbravská cesta 9, 84104 Bratislava, Slovakia
[2]Institute of Normal and Pathological Physiology, Slovak Academy of Sciences, Sienkiewiczova 1, 811 09 Bratislava, Slovakia
[3]Department of Cardiology, Slovak Institute of Cardiovascular Diseases, Pod Krásnou Hôrkou 1, 831 01 Bratislava, Slovakia

Abstract. High resolution body surface potential maps and an equivalent current dipole model of the cardiac generator were used to assess the heart state in two abnormal conditions: WPW syndrome with single accessory pathway and local ventricular ischemia. Results of a simulation study and experimental verification of the method for both cardiologic abnormalities are presented.

Single accessory pathway in WPW syndrome was simulated as initial ventricular activation at the atrio-ventricular ring. Using a current dipole model of the cardiac generator, the locus of arrhythmogenic tissue was assessed with a mean error of 11 mm. Experimental localization of the accessory pathway in a WPW patient was in good agreement with the invasively obtained site.

Local repolarization changes were simulated as shortening of the myocytes action potentials in three regions typical for stenosis of main coronary arteries. Using surface QRST integral maps and dipolar source model, small subendocardial and subepicardial lesions of myocardium were inversely located with a mean error of 9 mm and larger transmural lesions with a considerable mean error of 17 mm. Extent and prevalence of subepicardial or subendocardial type of the lesion were reflected in the dipole moment and orientation. In experimental verification of the method, in 7 of 8 patients that underwent PCI of a single vessel, estimated equivalent current dipole position matched well the treated vessel.

The results suggest that diagnostic interpretation of body surface potential maps based on dipolar source model could be a useful tool to assess local pathological changes in the heart.

Key words: body surface potential mapping, noninvasive cardiac diagnostics, equivalent current dipole model of the cardiac generator, ECG simulation.

1. Introduction

Aim of the presented study was to analyze the possibility of noninvasive identification of some local abnormal changes in the heart by evaluation of cardioelectric potentials measured on the chest surface using parameters of simple equivalent current dipole (ECD) model of the cardiac electric generator for characterization of the pathology. Two kinds of pathological situations were analyzed: WPW syndrome with single accessory pathway and small ischemic lesion in single vessel coronary heart disease.

Some types of cardiac arrhythmias have their origin in small confined areas of the myocardium. This is also the case of Wolff-Parkinson-White (WPW) syndrome where an abnormal conducting tissue (accessory pathway) exists between the atria and ventricles. The most precise localization of the arrhythmogenic substrate has been provided invasively during catheterization from electrograms measured directly in the heart during a radio-frequency catheter ablation procedure. However, noninvasive prediction of the location of the substrate could substantially shorten and simplify the invasive procedure. Noninvasive localization of the conducting pathway by evaluating body surface potential maps during the initial interval of the ventricular activation started at the site of the pathway, while the normal activation in other part of the ventricular volume still did not develop, was proposed in this study.

Shortening and decrease of action potentials (AP) is typical for ischemic cardiac cells. These subtle variations of AP influence the overall repolarization process and are expressed mainly in the ST-T interval of surface ECG signals. It was shown, that integrals of potentials over the ventricular depolarization – repolarization period (QRST interval in ECG) practically depend only on the action potentials variations and not on the ventricular activation sequence [1]. Differences in QRST integrals over the torso, displayed in difference QRST integral maps, together with the knowledge of geometry and electrical properties of the torso, thus can be used for a noninvasive identification of ischemic heart regions with changed repolarization.

2. Methods and material

Body surface potentials (BSP) simulated or measured in 24 to 198 chest surface points, dipole model of the cardiac electric generator as well as geometry and electrical properties of the inhomogeneous volume conductor of the human torso were used to assess specific characteristics of the heart state in two abnormal clinical conditions: (i) in WPW syndrome with sin-

*e-mail: tysler@savba.sk

gle accessory pathway and (ii) during local ischemic changes in the ventricular myocardium.

Site of single abnormal conductive pathway in WPW syndrome was localized by inverse computations from BSP during the initial interval of the ventricular depolarization. It was supposed that only small region around the accessory pathway was activated during this short interval hence single equivalent fixed current dipole was an appropriate model of the cardiac electric generator. Its position was searched at one of chosen possible sites along the atrio-ventricular ring by minimizing the rms difference between the original BSP and BSP generated by the dipolar generator.

Location of single ischemic lesion in some myocardial regions influenced by the stenosis of one of the coronary arteries was assessed using the difference between normal BSP and BSP obtained as a result of the shortening and/or decrease of the AP of cardiac cells in the ischemic lesion. Supposing a small lesion, this difference was interpreted as being caused by an additional dipolar source evoked by the AP difference during the whole repolarization phase. To reflect this fact, differences in integrals of surface potentials over a time interval containing the whole repolarization period were used to identify the lesion. Position of the dipole was searched among a set of possible locations within the ventricular volume by minimizing the rms difference between the original difference integral map and map generated by an ECD generator computed for each of the possible locations.

Relative rms deviation $RDev$ between values A_i of cardiac BSP data and values S_i of BSP generated by the equivalent dipolar source were evaluated to estimate the feasibility of the dipole source to represent the simulated or measured maps:

$$RDev = \frac{\sqrt{\sum_i (S_i - A_i)^2}}{\sqrt{\sum_i A_i^2}}$$

For both clinical abnormalities, the method was tested on simulated surface potentials and the influence of several error factors on accuracy of inverse procedures was analyzed to estimate their performance. A forward model was used to get well defined simulated body surface potentials in a normal case as well as in the two pathological cases. WPW syndrome with single accessory pathway was simulated by abnormal depolarization of the ventricles that was initiated in predefined positions along the atrio-ventricular ring. Local ischemia was simulated by areas with changed AP that were defined in different regions of the left ventricle. Finally, the method was experimentally tested on available data from WPW and ischemic patients.

2.1. Model of the cardiac electric generator. Equivalent cardiac generator based on single current dipole source located at one position selected from a set of predefined locations defined in the examined heart region was considered to characterize the accessory pathway or small ischemic region with changed repolarization. For each predefined location $i = 1, 2, \ldots n$, an ECD source representing the body surface potentials $\boldsymbol{\Phi}(t)$ was estimated using the formula:

$$\boldsymbol{D}_i(t) = \boldsymbol{T}_i^{+} \boldsymbol{\Phi}(t)$$

where $\boldsymbol{T}_i^{+}$ is pseudoinverse of a transfer matrix, $\boldsymbol{D}_i(t)$ are components of some ECD located at i-th location. Transfer matrix $\boldsymbol{T}_i$ represents the relation between position of the i-th dipole and the surface potentials and reflects the geometrical and electrical properties of the torso volume conductor. To solve the inverse problem of $\boldsymbol{D}_i$ estimation, pseudo-inverse $\boldsymbol{T}_i^{+}$ was obtained by singular value decomposition.

Minimal rms difference between original potentials and potentials generated by ECDs in all possible positions was used as a criterion to indicate the best, most probable position of the ECD source representing the initial ventricular activation or changed repolarization of ventricles.

To get more reliable and stable solutions, integral values of potentials $\boldsymbol{\Phi}(t)$ over a selected time interval were used instead of using instant values. Correspondingly, integrals of the dipole moments characterizing the evaluated interval were obtained.

Ventricular model with analytically defined geometry formed by several ellipsoides was used to define the bounded volume where the equivalent dipole had to be located [2].

In the WPW syndrome, initial interval of ventricular activation, typically from 7.5 to 25 ms was evaluated. This interval was selected to avoid evaluation of noisy data at the very beginning of the ventricular activation and later starting normal ventricular activation coming from the Purkinje conducting system. To define possible positions of the ECD, ventricular volume was divided into 39 segments, 16 of them along the atrio-ventricular ring (Fig. 1a) and the ECD generators were located in their gravity centers.

When analyzing small ischemic regions, only differences between surface potentials during normal and changed repolarization were evaluated for the whole QRST interval that includes also the repolarization period. In this case, possible changes in the depolarization sequence will not influence the integral of potentials $\boldsymbol{\Phi}(t)$ and both, decrease and shortening of the AP will be accounted in the ECD generator characterizing the changed repolarization. To assess the sensitivity of the method, possible positions of the ECD were defined at almost 300 vertices of a triangulated epicardial and endocardial surface of the ventricular model (Fig. 1b). However, for experimental verification on patients with no individual chest geometry data, coarser division of analytical (Fig. 1c) or realistic (Fig. 1d) ventricular volume to only 28 segments was used and possible positions of the ECD generator were placed in their gravity centers.

Accuracy of the inverse estimation of the ECD source representing the ischemic lesion is limited by the set of chosen dipole positions. Possible positions of the ECD should be chosen to adjust localization error on an acceptable level: less then supposed error of really obtainable geometry data and comparable with accuracy obtainable when using single moving dipole model [3]. In our simulations, the minimal distance be-

tween the nearest chosen position and correct location of an ECD generator (position of initial activation in WPW simulations or center of simulated ischemic lesion) was from 2 to 7 mm.

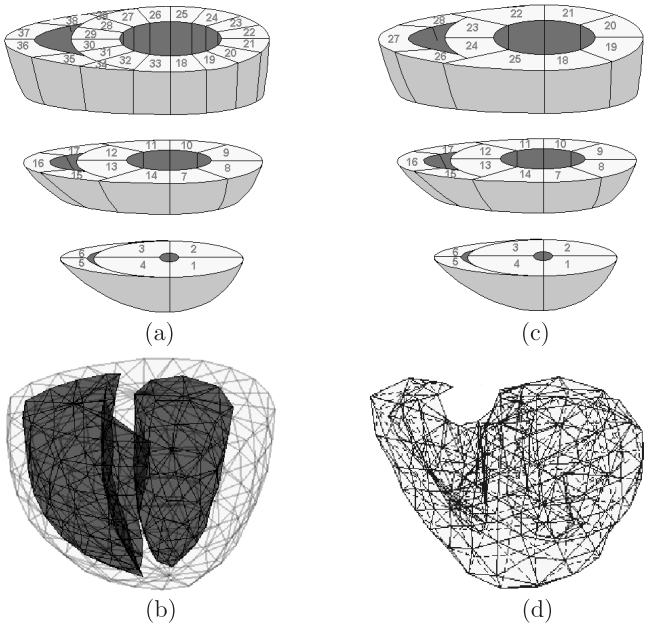

Fig. 1. Ventricular myocardium was divided into 39 segments for accessory pathway localization in the WPW syndrome (a), possible positions of the ECD were in gravity centers of the segments. Possible positions of ECD characterizing small ischemic lesions were defined at the vertices of epicardial and endocardial surface of the ventricular volume model (b). Analytical (c) or realistic (d) model of the ventricular myocardium divided into 28 segments was used for identification of local ischemia in patients without measured chest geometry, possible positions of the ECD were in gravity centers of the segments

2.2. Simulation of surface potentials during normal and abnormal heart activation. To simulate the surface potentials, forward model with three basic components was used: (i) finite element model of the heart ventricles, (ii) equivalent multiple dipole model of the cardiac electric generator and (iii) piecewise homogeneous torso model in which boundary element method was used for potential computation.

Finite element model of heart ventricles with element size of 1 mm^3 and with the same analytically defined geometry as for the ECD positioning was used to simulate the ventricular depolarization and repolarization [2]. Normal depolarization was started at points of early activation that were experimentally observed in normal human hearts. Spread of activation in isotropic myocardial tissue was governed by cellular automaton. A layer with three times increased conduction velocity was used at the endocardial surface to simulate the Purkinje fibers, up to five layers with different AP parameters were defined in the ventricular walls and in the septum (Fig. 2).

Linear AP shape was used to simulate the initial ventricular depolarization in WPW syndrome (Fig. 3a). To simulate the myocardium repolarization, realistic AP shapes (Fig. 3b) with different parameters in five layers from epicardium to endocardium were defined in ventricular walls and in the septum. Experimentally observed distribution of AP duration in the ventricular walls was preserved in the simulations, their transmural dispersion was about 40 ms with shorter AP duration at the epicardial surface and longest duration in the middle of the walls (modeling so called M-cells) [4,5].

Besides normal activation, also changed depolarization sequence in WPW syndrome and changed repolarization in small ischemic regions were simulated. To simulate different cases of WPW syndrome with single accessory pathway, ventricular depolarization was initiated in 8 physiologically defined regions on the epicardial surface along the atrio-ventricular ring [6] (Fig. 4).

Changed repolarization of ventricular myocardium during ischemia was modeled by shortening and/or decrease of AP by 5% to 20% from the normal values. Three typical regions of changed AP influenced by the stenosis of main coronary vessels were defined as shown in Fig. 5: antero-septal part of the left ventricle near the apex (supplied by left anterior descending coronary artery, LAD), postero-lateral part of the left ventricle close to the heart base (supplied by circumflex coronary artery, Cx) and mid postero-septal left and right ventricle (supplied by right coronary artery, RCA). In each region, smaller subepicardial and subendocardial lesions (3 – 8% of the ventricular volume) and larger transmural lesions (10 – 12% of the ventricular volume) were simulated.

To make the computation of surface potentials easier, multiple dipole model having 168 segmental dipoles was used to represent the cardiac electric generator. Each of these segmental dipoles was obtained as a sum of elementary dipoles in one of 168 anatomically defined myocardial segments.

Boundary element method was employed to compute potentials on the surface of a realistic inhomogeneous torso model (Fig. 6a) comprising lungs and ventricular cavities with conductivities equal to 0.25 and 3.0 times the torso conductivity, respectively.

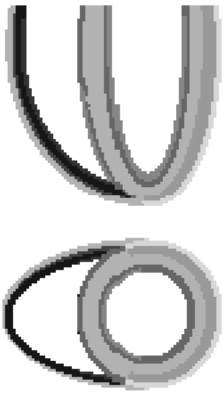

Fig. 2. Analytically defined ventricular volume composed of ellipsoids with endocardial conductive layer simulating the Purkinje fibers and with up to five layers of elements having different amplitudes and durations of action potentials

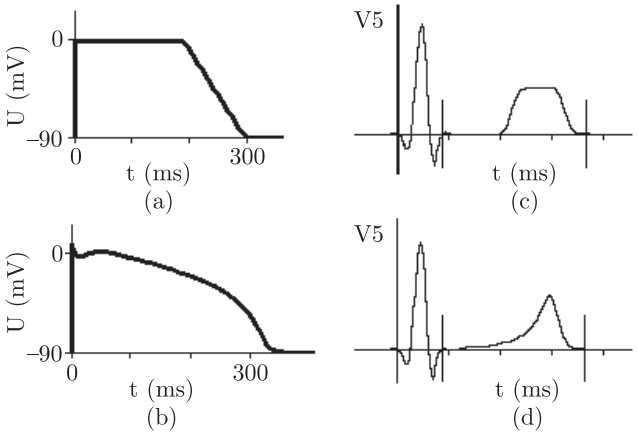

Fig. 3. Linear (a) and realistic (b) shape of the action potentials used in the study and their influence on the simulated surface ECGs (c and d, respectively)

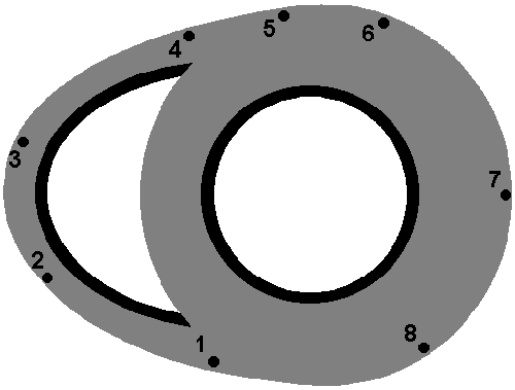

Fig. 4. Simulated positions of single accessory pathway along the atrio-ventricular ring: 1 – anterior septal, 2 – anterior RV, 3 – lateral RV, 4 – posterior RV, 5 – posterior septal, 6 – posterior LV, 7 – lateral LV, 8 – anterior LV

Fig. 5. Ventricular myocardium model with regions of changed repolarization. Left: antero-septal regions in the LV; center: postero-lateral regions in the LV; right: inferior regions in the mid postero-septal LV and RV. Cuts are led through the lesion centers, several sizes of lesions are marked by different grey levels

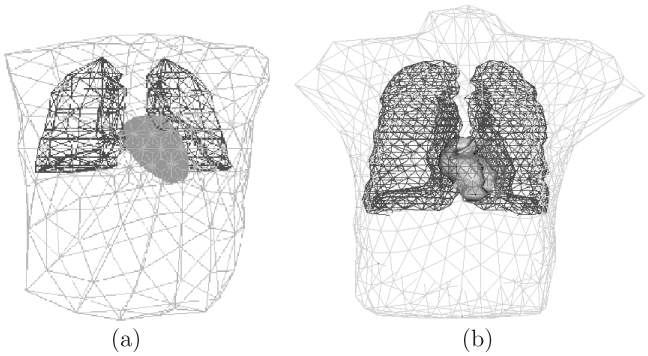

Fig. 6. a) Inhomogeneous human torso with realistically shaped chest and lungs and analytical heart geometry was used in the forward and inverse computations as a common torso model, b) real individual chest geometry obtained from CT was used for accessory pathway localization in the WPW patient

2.3. Simulation of error factors. Influence of selected factors causing error in identifying the studied pathologies was analyzed. Incomplete knowledge of the thorax geometry was represented by neglecting of lungs and heart cavities and using homogeneous torso model. Errors in determination of the heart position were simulated by shifts and rotations of the equivalent cardiac generator (misplacements of heart points predefined as possible locations of the accessory pathway were about 1 cm). Noise with normal distribution and standard deviation 3–30 μV was added to simulated surface potentials. Accuracy of inverse computations from potentials simulated in 198 points defining the whole surface of the model torso and in several practically used mapping lead sets with 24 to 63 unipolar leads was estimated by mean error of the accessory pathway localization.

2.4. Verification on real data. Identification of single accessory pathway was attempted on a WPW patient measured by Shadidi et al. [7]. ECG potentials from 63 mapping leads and the shape of thorax with lungs and ventricles including cavities based on CT scans (Fig. 6b) were used in the inverse computations. Intraoperative measurements of epicardial potentials located the preexcitation site at the base of the lateral wall of the left ventricle. To test the influence of incomplete geometry knowledge on the inverse computations, both, individual chest geometry obtained from CT (Fig. 6b) and model chest, the same one as used in the forward potential simulations (Fig. 6a), were used in the study [8].

Identification of local repolarization changes was tested on available data from 11 MI patients (age 45–69, 8 men and 3 women) that underwent successful PCI (percutaneous coronary intervention) treatment of single vessel (8 LAD, 1 Cx, 2 RCA) [9]. QRST integral maps before and after the intervention were computed in a 12×16 grid, mapped surface potentials were estimated from 32 measured ECG leads as suggested by Lux et al. [10]. Values in maps were corrected for QT interval length if it varied more than 5% between the measurements. Common realistic inhomogeneous torso model (Fig. 6a) with both, analytical or realistic heart geometry as shown in Figs. 1c and 1d were used in all patients to localize an ECD representing the region with changed repolarization.

3. Results

3.1. Assessment of accessory pathway in WPW syndrome. Mean errors of the accessory pathway localization using simulated BSP and several ECG lead sets are shown in Table 1. When none of the analyzed error factors was present in the input data, all lead sets enabled acceptable localization of the accessory pathway; mean error increased from about 0.5 to 0.9 cm when number of measured leads decreased from 198 to 24. Slightly higher errors 0.5 to 1.0 cm were obtained when homogeneous torso model was used.

ECG noise in wide range between 3 to 30 μV rms did not influence the localization error when BSP were measured over the whole torso using 198 points or 63 mapping leads. For limited number of leads and noise above 10 μV rms, the localization error increased, e.g. for 24 leads it reached 0.7 cm.

When accessory pathway was localized from 63 leads, neglect of torso inhomogeneities was reflected in an increased mean localization error to about 0.8 cm. Influence of the heart misplacement caused by unknown precise heart position was simulated by heart shifts and rotations resulting in displacement of the accessory pathway about 1 cm. These displacements were projected into a mean localization error of the same magnitude. Combination of all analyzed error factors resulted in a mean localization error of about 1.1 cm (Table 2).

Table 1
Influence of the lead set on the mean error of the accessory pathway localization

Lead set, number of leads	Mean error of pathway localization (cm)	
	Inhomogeneous torso	Homogeneous torso
Torso 198	0.5	0.6
Savard 63	0.5	0.8
Lux 32a	0.4	0.5
Barr 24	0.9	1.0

Table 2
Errors of accessory pathway localization from 63 leads. Simulated influence of several error factors and their combination

Error factors	Number of simulations	Mean localization error (cm)
No	8	0.5
Noise 5 μV rms	40	0.5
Homogeneous torso	8	0.8
Heart misplacements ∼ 1 cm	40	1.0
Combined factors	200	1.1

For the WPW patient, 63 leads ECG measurements and several torso geometry configurations were tested in the inverse computations. If real inhomogeneous torso shown in Fig. 6b) was used, it was possible to locate the accessory pathway within 1 heart segment. The accessory pathway site was satisfactorily located (Fig. 7) even if real, but electrically homogeneous torso or both, inhomogeneous or homogeneous torso models were used (Table 3).

Table 3
Segments with localized accessory pathway in a patient measured in 63 ECG leads. Actual site of accessory pathway was in segments 19–21, see Fig. 1a

Torso geometry	Identified segment number in the heart	
	Inhomogeneous torso	Homogeneous torso
Real	19	19
Model	19	20

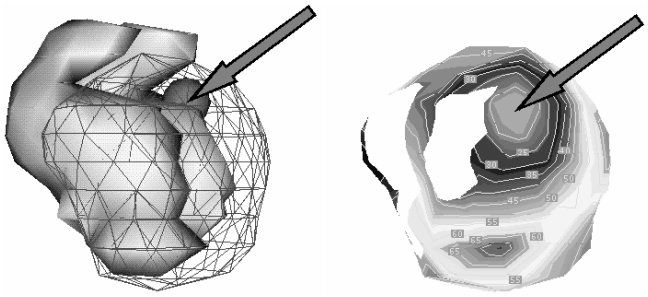

Fig. 7. Site of non-invasively localized accessory pathway in a WPW patient when real chest and heart geometry were used (left) and published site [after Ref. 11] obtained for the same patient when uniform double layer model of the cardiac generator was used (right)

3.2. Assessment of local repolarization changes in ischemia. Difference QRST body surface integral maps were used for identification and localization of small heart regions with changed repolarization. All changes in antero-septal and postero-lateral LV regions as well as in postero-septal (inferior) regions in LV and RV were clearly projected to surface integral maps and typically located changes were visible in corresponding locations over the torso surface.

In Fig. 8 there is an example of simulated normal QRST integral map and maps obtained if AP was shortened by 20% in antero-septal LV, postero-lateral LV and postero-septal LV and RV regions of medium size (regions A2, P2, I2). AP shortening was projected as decrease of the QRST integral mainly on the near-by left anterior, mid posterior and lower right anterior and posterior torso surface, respectively.

Relative rms differences between simulated normal and changed QRST integral maps were 20–45% rms and were proportional to the AP changes. However, these differences did correspond with the lesion size only for subendocardial regions while large transmural regions produced smaller differences with flatter extremes than medium subendocardial lesions. Differences obtained by modelling of AP changes in the antero-septal part of the LV are demonstrated in Fig. 9. Similar results were obtained in other ventricular regions.

Results of the inverse solution using 62 surface leads and homogeneous or inhomogeneous torso model are summarized in Table 4. Relative rms deviations between original difference QRST integral maps and equivalent dipolar maps were from 9 to 16% and suggest that ECD may be an adequate representation namely of small ischemic lesions.

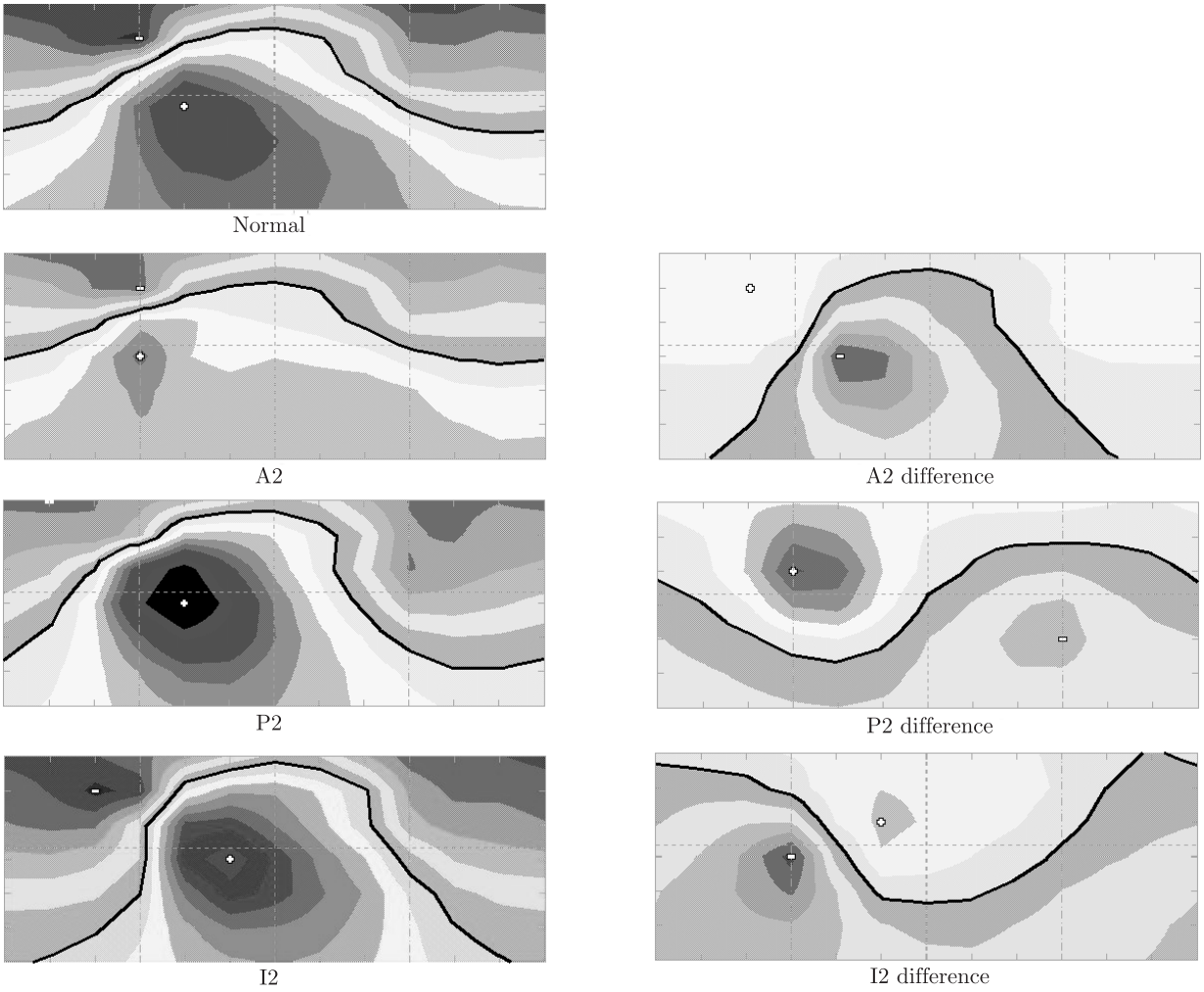

Fig. 8. Simulated QRST integral maps (left column) for normal depolarization-repolarization (Normal) and for activations with AP shortened by 20% in lesions of medium size located in antero-septal (A2), postero-lateral (P2) and postero-septal (I2) part of the ventricular myocardium. Corresponding difference QRST integral maps are shown in the right column. Steps in maps are 6 mV.ms, starting from the marked zero line

Table 4
Errors (mean ± standard deviation) of the inverse identification of small subendo- or subepicardial lesions and larger transmural lesions from 62 surface ECG leads and using inhomogeneous or homogeneous torso model

Evaluated parameter	Torso model	Small lesions	Large lesions
Localization error (mm)	inhomogeneous	9 ± 4	17 ± 14
	homogeneous	11 ± 8	16 ± 15
Dipole direction (°)	inhomogeneous	9 ± 7	14 ± 4
	homogeneous	8 ± 5	17 ± 7
Dipole moment (%)	inhomogeneous	51 ± 40	221 ± 206
	homogeneous	49 ± 33	163 ± 123
Map relative difference (%)	inhomogeneous	9 ± 4	16 ± 1
	homogeneous	12 ± 2	16 ± 2

For small subendocardial and subepicardial lesions, maximal localization error reached 16 mm (23 mm in homogeneous torso). Localization of large transmural lesions was less satisfactory and maximal error reached unacceptable 43 mm. Orientation of the ECDs matched well the simulated lesions, however, relative error of dipole moments substantially increased for more distributed sources, especially for large transmural lesions. Figure 10 illustrates the comparison between original dipolar representation (full line vector) and inversely calculated equivalent dipole (dashed line vector) representing simu-

lated small subendocardial lesions A2, P2 and I2 in the antero-septal wall of the LV, postero-lateral wall of the LV and in the mid postero-septal LV and RV, respectively.

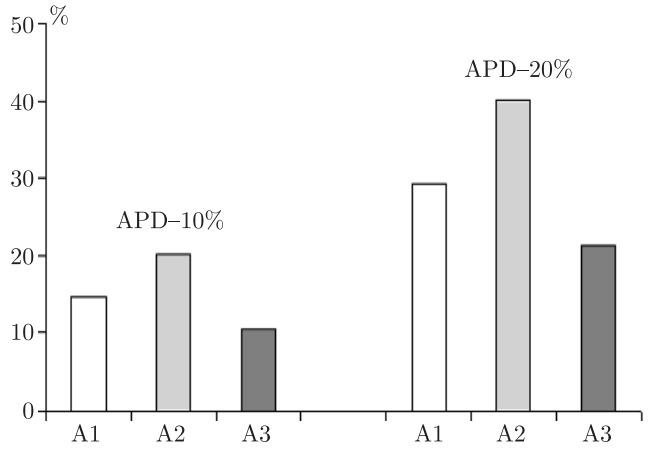

Fig. 9. Relative rms difference between normal and changed QRST integral maps for AP shortening by 10% and 20% in lesions A1, A2, A3 of three different sizes located in antero-septal region of the LV and shown in Fig. 5. Their sizes were 3, 6 and 10% of the ventricular volume, first two lesions were subendocardial, the last one was transmural

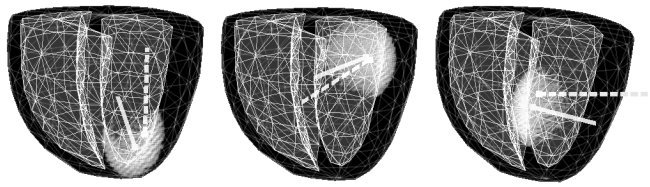

Fig. 10. Examples of simulated ischemic lesions and their dipolar representations. Representing dipoles computed as sum of simulated elementary dipoles in the lesion are marked by full line vectors, inversely calculated equivalent dipoles are marked by dashed line vectors. Left: A2 lesion the in antero-septal wall of the LV; center: P2 lesion in the postero-lateral wall of the LV; right: I2 lesion in the mid postero-septal part of the LV and RV

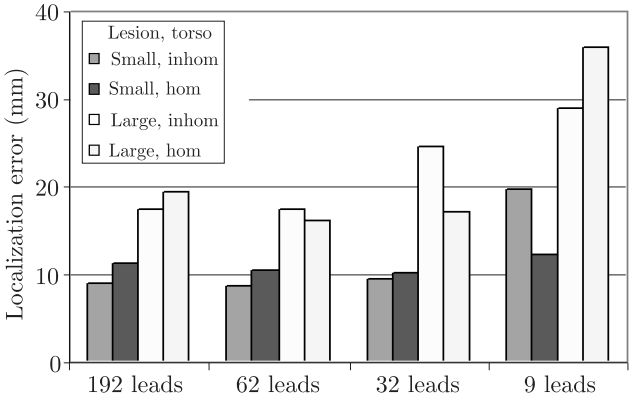

Fig. 11. Mean values of the localization error (mm) for small subendo- or subepicardial lesions and for large transmural lesions when using different lead sets and homogeneous or inhomogeneous torso models

Localization of small lesions from 192 and 62 leads provided similar results, localization from 32 leads was slightly worse, while localization from 9 leads was not satisfactory. For larger lesions, influence of the number of leads was generally higher. In most cases, results obtained using homogeneous torso model were less accurate than those obtained when inhomogeneous torso model was used. Detailed results are illustrated in Fig. 11.

In 8 of 11 studied MI patients we have found significant changes in QRST integral maps after the PCI treatment that could be approximately represented by a single dipole (in 6 cases the relative rms error of the dipolar representation of the difference integral map was less than 35%, in 2 another cases it was about 50%). In remaining 3 patients the error was $> 60\%$ and they were excluded from further analysis. In 6 of 8 analyzed patients QT interval correction was used to compensate for the changed heart rate between the measurements.

Despite the use of a common torso model, in 7 of the 8 analyzed patients the positions of estimated equivalent dipoles approximately matched the region supplied by the treated vessel or at least they were correctly located at anterior or postero-lateral wall of the LV. Directions of dipole moments in several cases were not normal to the particular heart wall what might reflect specific form of the affected area. In 1 patient after PCI on RCA, the equivalent dipole was located in mid anterior LV wall with a dipole moment directed out of the heart volume. In Fig. 12 there is an example of measured patient data and successful location of the ECD after PCI on LAD.

4. Discussion and conclusions

Presented simulation results suggest that high resolution BSP data together with known patient torso geometry can be used for noninvasive assessment of pathological heart states in selected situations. However, some limitations of the study have to be taken into account. Because of the limitations of the model, validity of the obtained results has to be thoroughly verified on patient data.

The main limitation of the forward model is the simple heart geometry without atria and use of isotropic myocardium. Further, action potential shapes and durations in the myocardium elements were defined *apriori* and their possible mutual influence (electrotonic coupling) was not simulated. Therefore, careful adjustment of AP duration and other AP characteristics was necessary to obtain realistic simulated potentials. All these factors may cause inaccuracy of simulated surface potentials that should be considered when interpreting the results.

In real situations, the identified events, namely the local repolarization changes, can be masked by other physiological fluctuations and noise in measured data. Difference integral maps should be corrected to suppress known physiological variability (e.g. different heart rate before and after exercise test).

Our attempt to detect corresponding changes in BSP using departure integral maps showed that these changes are relatively small when compared with normal inter-individual fluctuations and can hardly be detected by departures from mean

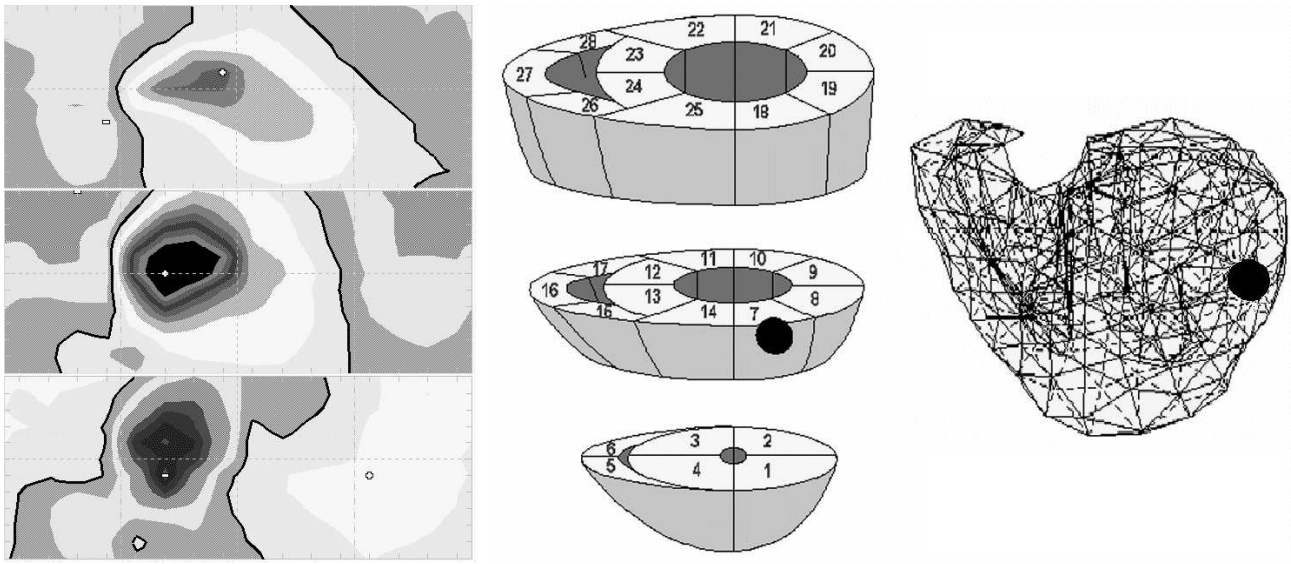

Fig. 12. QRST integral maps (steps in maps 12 mV/ms, starting from the marked zero line) measured before PCI and after PCI on LAD together with the corresponding difference integral map (left, top to bottom) in a 69 year old woman with anterior MI (95% stenosis on LAD). Localization of an equivalent dipole source representing the changed repolarization in an analytical (center) and realistic (right) myocardium model

normal integral maps. Moreover, transmural lesions produce less difference in the maps and their identification is more difficult. For larger lesions, single dipole model is probably not adequate and the localization may not be in correspondence with the real lesion position.

Only detection of AP duration changes during repolarization was presented in this study. Simultaneous changes of AP amplitudes that are present in real ischemia were also tested on the model and corresponding simulations confirmed similar effect of both, AP shortening and amplitude decrease, on the integral maps.

Despite the limitations of this study, presented results indicate that model based methods might be able to determine the position of single accessory pathway in WPW syndrome within one of 16 regions along the atrio-ventricular ring with acceptable localization error if at least 63 ECG leads are measured, realistic torso geometry is used, noise in ECG is reasonably low (less than 30 μV) and inaccuracy of the heart position is less than 10 mm. Mean localization error about 1.1 cm can be expected.

Presented localization of single accessory pathway from 63 measured leads in a real patient using individual torso geometry was in good agreement with the invasively obtained site [7] as well as with published data obtained by a different method [11].

Results of the simulations also suggest that local repolarization changes in different heart regions could be observed in changed QRST integral maps. Relative rms differences between simulated normal and changed QRST integral maps were 20–45% rms, correlations 0.45–0.99. These were greater than observed total intra-individual variability in maps in healthy subjects (5–20% rms, correlations > 0.98) what, in principle, allows their identification. In most measured patients, difference between normal and changed integral maps (for example before and after an exercise test or during repeated measurements over a long time period) could be used to localize the ECD source corresponding to the small region of changed repolarization.

Acknowledgements. This work was supported by grants 2/4089/24 and 2/3203/25 from the VEGA grant agency.

References

[1] V. Szathmáry and I. Ruttkay-Nedecký, "Effects of different sources of ventricular repolarization heterogeneity on the resultant cardiac vectors. A model study", *Health Data in the Information Society. Proceedings of MIE2002*, 88–92 (2002).

[2] V. Szathmáry and R. Osvald, "An interactive computer model of propagated activation with analytically defined geometry of ventricles", *Comput. Biomed. Res.* 27, 27–38 (1998).

[3] R. Hren, G. Stroink, and B.M. Horacek, "Accuracy of single-dipole inverse solution when localising ventricular preexcitation sites: simulation study", *Med. Biol. Eng. Comp.* 36, 323–328 (1998).

[4] G.X. Yan, W. Shimizu, and Ch. Antzelevich, "Characteristics and distribution of M cells in anterially perfused canine left ventricular wedge preparations", *Circulation* 98, 1921–1927 (1998).

[5] G.R. Li, J. Feng, L. Yue, and M. Carrier, "Transmural heterogeneity of action potentials and Ito1 in myocytes isolated from the human right ventricle", *Am. J. Physiol.* 275, H369–H377 (1998).

[6] M. Tyšler, M. Turzová, M. Tiňová, and J. Švehlíková, "Accuracy evaluation of non-invasive localization of accessory pathways", *Biomedizinische Technik* 42 (1), 281–284 (1997).

[7] A.V. Shahidi, P. Savard, and R. Nadeau, "Forward and inverse problems of electrocardiography: modeling and recovery of epicardial potentials in humans", *IEEE Trans. Biomed. Eng.* 41, 249–256 (1994).

[8] M. Tiňová, M. Tyšler, and M. Turzová "Inverse localization of preexcitation sites using a jumping dipole", *Journal of Electrocardiology* 30, 348 (1997).

[9] M. Tysler, M. Turzova, and S. Filipova, "Assessment of local repolarization changes using model based BSPM interpretation", *Advances in Electrocardiology 2004*, 158–162 (2005).

[10] R.L. Lux, C.R. Smith, R.F. Wyatt, and J.A. Abildskov, "Limited lead selection for estimation of body surface potential maps in electrocardiography", *IEEE Trans. Biomed. Eng.* 25, 270–276 (1978).

[11] G.J.M. Huiskamp, T. Oostendorp, N.H.J. Pijls, and A. van Oosterom, "Invasive confirmation of the human ventricular activation sequence as computed from body surface potentials" *Computers in Cardiology '92*, (1992).